https://doi.org/10.5194/esd-2019-57
Preprint. Discussion started: 26 September 2019

Earth System Dynamics Discussions
Open Access
EGU

On the time evolution of ENSO and its teleconnections in an ensemble view – a new perspective

Tímea Haszpra[1,2,†], Mátyás Herein[1,2,†], and Tamás Bódai[3,4]

[1]Institute for Theoretical Physics, Eötvös Loránd University, Budapest, Hungary
[2]MTA–ELTE Theoretical Physics Research Group, Eötvös Loránd University, Budapest, Hungary
[3]Pusan National University, Busan, Republic of, Korea
[4]Center for Climate Physics, Institute for Basic Science, Busan, Republic of Korea
[†]These authors contributed equally to this work.

Correspondence: hatimi@caesar.elte.hu

Abstract. The changes in the El Niño–Southern Oscillation (ENSO) phenomenon and its precipitation-related teleconnections over the Globe under climate change are investigated in the Community Earth System Model's Large Ensemble from 1950 to 2100. For the investigation, a recently developed ensemble-based method, the snapshot empirical orthogonal function (SEOF) analysis is used. The instantaneous ENSO pattern is defined as the leading mode of the SEOF analysis carried out at a given time instant over the ensemble. The corresponding principal components (PC1s) characterize the ENSO phases. We find that the largest amplitude changes in the variability of the sea surface temperature fields occur in the June–July–August–September (JJAS) season, in the Niño3–Niño3.4 region and in the eastern part of the Pacific Ocean, however, the increase is also considerable along the Equator in December–January–February (DJF). The Niño3 amplitude shows also an increase of about 20% and 10% in JJAS and DJF, respectively. The strength of the precipitation-related teleconnections of the ENSO is found to be non-stationary, as well. For example, the anti-correlation with precipitation in Australia in JJAS and the positive correlation in Central and North Africa in DJF are predicted to be more pronounced by the end of the 21th century. Half-year-lagged correlations, aiming to predict precipitation conditions from ENSO phases, are also studied. The Australian, Indonesian precipitation and that of the eastern part of Africa in both JJAS and DJF seem to be well predictable based on ENSO phase, while the South Indian precipitation is in relation with the half-year previous ENSO phase only in DJF. The strength of these connections increases, especially from the African region to the Arabian Peninsula.

1 Introduction

The El Niño—Southern Oscillation (ENSO) is recognized as the dominant interannual fluctuation in the climate system (see, e.g., Bjerknes, 1969; Rasmusson and Carpenter, 1982; Neelin et al., 1998; Philander, 1990; Timmermann et al., 2018). This naturally occurring fluctuation originates in the tropical Pacific region and affects weather and climate worldwide. The warm (cold) phase of the ENSO, called El Niño (La Niña), is associated with above (below) average sea surface temperature in the central and eastern equatorial part of the Pacific Ocean. The ENSO cycle also has several regional impacts on precipitation and temperature over the Globe. For example, during El Niño episodes Australia, Indonesia in both December–February and

https://doi.org/10.5194/esd-2019-57
Preprint. Discussion started: 26 September 2019

Earth System Dynamics Discussions
Open Access
EGU

June–September, and India and the equatorial band in Africa in December–February experience a reduced amount of rainfall, while Peru and Chile has wetter than normal weather in July–September (see, e.g., Diaz et al. (2001); Yang and DelSole (2012); Yeh et al. (2018)).

Therefore, if the ENSO changes it may have large climatic impacts (Trenberth et al., 1998; Wallace et al., 1998; Glantz et al., 2001; Trenberth et al., 2002; Guilyardi et al., 2009; Collins et al., 2010; Vecchi and Wittenberg, 2010; Cai et al., 2015). Consequently, an open and crucial question is how ENSO will change in the changing climate. There has been many studies aiming to answer this question, however, the model simulations of future ENSO changes diverge widely among climate models (Yeh and Kirtman, 2007; Stevenson, 2012; Christensen et al., 2013; Bellenger et al., 2014).

Most of the studies agree on using temporal statistics (including means, variances, correlations, etc.) applied to a time-dependent dynamical system, i.e., in our changing climate. However, a correct application of temporal statistics requires stationarity, as argued in Drótos et al. (2015, 2016), which does not hold in a changing climate. The non-stationarity of the climate system naturally appears in the simulations generated for climate projections by general circulation models, and it is especially important in the analysis of teleconnections (Herein et al., 2016, 2017; Roy et al., 2019; Chung et al., 2019).

To avoid the above-mentioned contradiction, in this study we present an ensemble-based analysis. In this approach the relevant quantities of the climate system are the statistics taken at any given time instant over an ensemble of possible climate realizations. These ensembles typically evolve from slightly different initial conditions. In the context of climate, this kind of ensembles was used, e.g., in Deser et al. (2012); Daron and Stainforth (2013); Kay et al. (2015); Stevens (2015); Bittner et al. (2016); Herein et al. (2016, 2017); Hedemann et al. (2017); Suarez-Gutierrez et al. (2018); Li and Ilyina (2018); Chung et al. (2019), as well as, large ensemble simulations were investigated in low-dimensional systems (see, e.g. Bódai et al., 2011; Bódai and Tél, 2012; Drótos et al., 2015). The application of ensembles in the snapshot framework is overviewed in Tél et al. (2019). The mathematical concept that provides the appropriate framework is that of snapshot (Romeiras et al., 1990; Drótos et al., 2015) or pullback attractors (Arnold, 1998; Ghil et al., 2008; Chekroun et al., 2011). The applicability of this framework was also established by laboratory experiments (Vincze et al., 2017).

In the context of climate simulations, this framework implies that a climate simulation with any initial condition after a transient time converges (during which it forgets its initial condition), to the snapshot attractor which describes the "permitted" climate states under the instantaneous forcing, such as CO_2 concentration, etc. Furthermore, starting a sufficiently large ensemble of climate simulations with slightly different initial conditions is proved to correctly cover the distribution of the possible climate states of the snapshot attractor after the transient time at any time instant, therefore, from that time on the ensemble can be used to characterize the potential states at each time instant (Drótos et al., 2015; Herein et al., 2016; Drótos et al., 2017). This ensemble can be also called parallel climate realizations (Herein et al., 2017; Tél et al., 2019). We note that it is remarkable that Leith (1978) came up with a similar idea as early as in 1978, however, Leith's work has not spread widely in the climate community.

This approach also provides a mathematically correct method to separate the effect of internal variability from the forced response under climate change (see, e.g. Drótos et al., 2015), via, e.g., the ensemble standard deviation and the ensemble mean, respectively. Naturally, due to the time-dependence of the forcing, i.e., when the climate changes, the ensemble also undergoes

https://doi.org/10.5194/esd-2019-57
Preprint. Discussion started: 26 September 2019


Earth System Dynamics Discussions
Open Access
EGU

a change in time, and as a consequence, both the mean state (average values) and the internal variability of the climate changes with time.

The snapshot framework can be applied also to phenomena analyzed by the widely used empirical orthogonal function (EOF) analysis. Here we use a recently developed approach called the snapshot EOF analysis (SEOF) to reveal the potential changes in the ENSO and its teleconnections. This method has been introduced originally in Haszpra et al. (2019). It computes instantaneous SEOF loading patterns over the ensemble members at any given time instant, rather than with respect to the time dimension of any single ensemble member. Hence it is also capable of monitoring the time-dependence of the SEOF pattern. We note that a similar method (called EOF-E) has also been developed recently in Maher et al. (2018), however, it differs from our SEOF method as it computes the EOF field for a given year partially over the ensemble dimension but constructing the sampling set from the different ensemble members and also from the different monthly fields of the given year with the seasonal mean signal previously removed.

This study focuses on the time evolution of the ENSO pattern and ENSO amplitude under the changing climate. Another crucial question is how ENSO teleconnections will be modified in the same time. Many studies have addressed this question and reported that the ENSO teleconnections may change under the changing climate (Kumar et al., 1999; Yeh and Kirtman, 2007; Davey et al., 2014; Ramu et al., 2018; Yeh et al., 2018). However, most of the studies use the before-mentioned temporal statistic approach to get the relevant correlation coefficients of teleconnections, which introduces some subjectivity due to the choice of the time-window over which statistics are taken. This subjectivity was investigated, e.g., in Herein et al. (2017), in which it has been demonstrated that the traditional evaluation of correlation coefficients, carried out via temporal statistics, provides incorrect or misleading results. Thus we emphasize that it is important to evaluate correlation coefficients and any other statistics with respect to the ensemble using the snapshot framework.

The SEOF method, computing all relevant quantities at single time instants, via the computed principal components (PC1s) of the leading SEOF mode used as certain ENSO indices to characterize the ENSO phases, also allows us to investigate ENSO teleconnections based only on instantaneous ensemble statistics. Since this can be done at any time instant it also enables us to monitor the temporal evolution of the strength of the teleconnection during a climate change.

We also compute instantaneous correlation coefficients to characterize the connection of the ENSO phases with precipitation over the Globe at each year, and investigate the trends in the obtained correlation coefficient maps. Lagged correlations between the two quantities can also be studied this way, providing the possibility of predicting precipitation half a year in advance based on PC1. We focus on the December–January–February (DJF) and the June–July–August–September (JJAS) season (for details see Data and Methods). In this way, in contrast to Maher et al. (2018) who uses all monthly data from a year, also the seasonal differences in the phenomenon can be investigated. We note that the SEOF method or any similar technique (e.g. EOF-E) can be applied successfully, providing robust statistics, only for large ensembles, at least with 30-40 members (Maher et al., 2018). Here, we choose to investigate the ENSO phenomenon in the large ensemble of one of the state-of the-art climate models, in the Community Earth System Model Large Ensemble Project (CESM-LE) (Kay et al., 2015). We emphasise that to our knowledge, this is the first time when the SEOF analysis using SST data was utilized to reveal changes in ENSO teleconnections.

https://doi.org/10.5194/esd-2019-57
Preprint. Discussion started: 26 September 2019


Earth System Dynamics Discussions
Open Access
EGU

The paper is organized as follows. Sect. 2 provides a brief overview of CESM-LE data and of the SEOF method. Sect. 3 presents the sea surface temperature regression maps as ENSO patterns, the ENSO amplitude and their changes due to climate change. The precipitation-related teleconnections of the ENSO phenomenon and the modifications of their strength are also discussed in the section. Sect. 4 summarizes the main results and conclusions of the work.

2 Data and Methods

For our study we use the meteorological fields of the CESM-LE produced by the fully-coupled CESM1 used in CMIP5 (Kay et al., 2015). Between 1920 and 2005 the CESM-LE simulations follow the CMIP5 historical experimental design (Taylor et al., 2012; Lamarque et al., 2010), while after 2005 to 2100 they follow the RCP8.5 scenario (Van Vuuren et al., 2011). In the study we utilize sea surface temperature (SST) and total precipitation (PRECT) fields with a horizontal resolution of $1^\circ \times 1^\circ$ and $1.25^\circ \times 0.942^\circ$, respectively. Due to the small systematic difference between the members run at NCAR and at the Toronto supercomputer (CESM-LE, 2016) we utilize only the members from the NCAR simulations. Taking into consideration the convergence time of the simulations we only deal with data from 1950 on.

Here, we study ENSO by evaluating the variability of the SST field over the ensemble members at each time instant in the Pacific using the SEOF method. It is based on the region of [30°S, 30°N]×[100°E, 70°W], which is also chosen in Maher et al. (2018) to their EOF-E analysis. On a "time instant" we mean seasonal average: note that a season can be considered short, but the snapshot framework is also applicable for quantities evaluated over time intervals (Drótos et al., 2015). To eliminate the distorting impact of the regular latitude–longitude grid in the EOF analysis, the SST fields are weighted by the square root of the cosine of the latitude following Thompson and Wallace (2000). We consider the instantaneous ENSO loading pattern as the leading SEOF mode, and the phase of the phenomenon in each member as the corresponding principal component (PC1). With the sign of the SEOF patterns which shall be used in Fig. 1 PC1> 0 (PC1< 0) corresponds to anomalously warm (cold) events associated with above (below) average SST in the central and east-central equatorial Pacific Ocean. As in Thompson and Wallace (2000) not the normalized EOF patterns, rather the SST regression maps are shown computed by regressing the unweighted SST anomaly fields onto the standardized PC1 data. Therefore, the values appearing on the regression maps characterize typical amplitudes in the variability of the SST. The instantaneous strength of the ENSO is computed as the ensemble standard deviation of the PC1s of the given time instant. For comparison, we also analyze the time evolution of the ENSO Niño3 amplitude defined by the standard deviation of SST in the [5°S, 5°N]×[150°W, 90°W] Niño3 region.

Note that PC1 is actually an index for the ENSO phase. It is closely related to the standard Niño3 (Ashok et al., 2007) and Niño3.4 indices (Takahashi et al., 2011) and has been used in this quality in other studies as well, see, e.g., Diaz et al. (2001) who carried out traditional EOF analysis using a slightly smaller Pacific region. As an index, its main use is a standardized indication for the state of the remote phenomena related to ENSO.

For characterizing such teleconnections, an instantaneous correlation coefficient can be determined between the PC1 and PRECT data of the ensemble members at each time instant and for each grid point. We utilize both DJF-mean and JJAS-mean data in order to reveal simultaneous and lagged connections, and correlate the JJAS PC1 with JJAS PRECT, the DJF PC1 with

https://doi.org/10.5194/esd-2019-57
Preprint. Discussion started: 26 September 2019

Earth System Dynamics
Discussions
Open Access
EGU

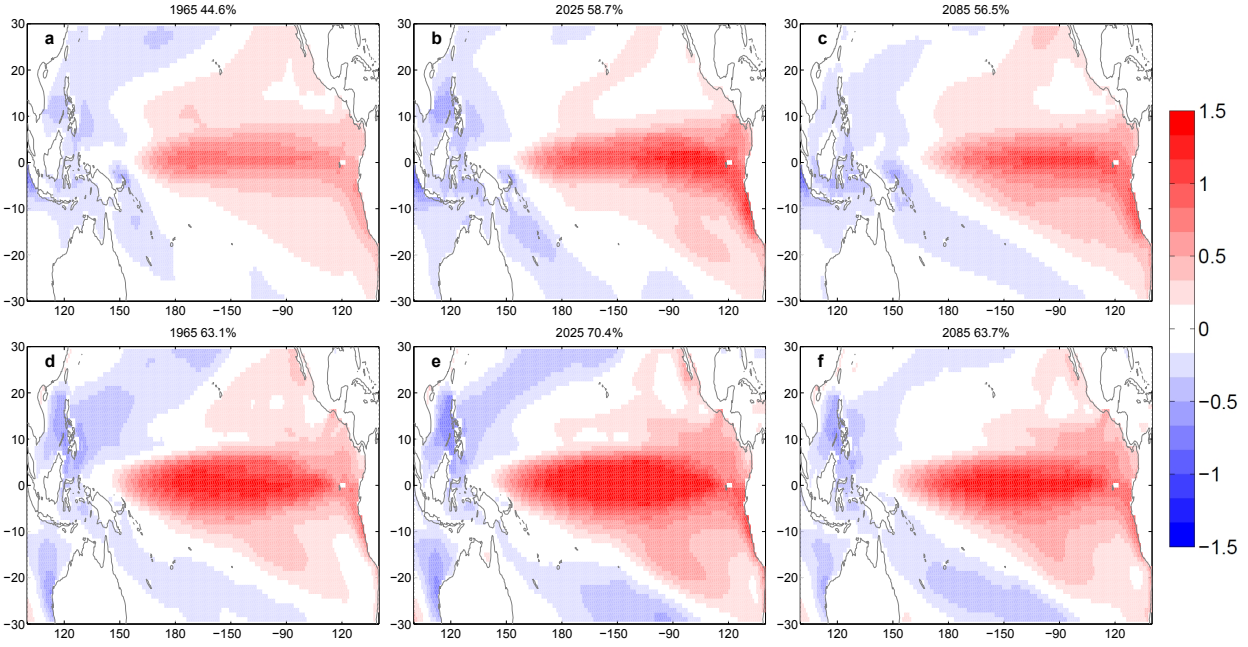

Figure 1. Ensemble-based SST regression maps [°C] for years given in the panel's title for JJAS (a-c) and DJF (d-f). The explained variance of the first SEOF mode is also displayed in the title of the panels.

DJF PRECT, the DJF PC1 with JJAS PRECT, and JJAS PC1 with DJF PRECT. The investigation of lagged correlations opens the possibility of studying the predictability of the amount of precipitation in different regions based on the PC1.

3 Results

3.1 Changes in the ENSO pattern and amplitude

For a first impression of the SEOF analysis, the instantaneous regression maps of the first SEOF mode for the SST in the Pacific region for the JJAS period and DJF period are shown in Fig 1.a-c and Fig 1.d-f, respectively. As expected from observation-based data, the SST variability is somewhat stronger in DJF than in JJAS, since the largest SST anomalies are known to be the strongest in the DJF season (see, e.g., Kirtman and Shukla, 2000). The shape of the pattern clearly changes somewhat over time and the explained variance of the first SEOF mode also varies.

To determine whether the observed alterations are due to fluctuations because of the finite number of ensemble members or the consequences of the changing climate, a linear fit is performed on the regression maps at each grid point (Fig 2). For JJAS (Fig 2.a) a positive trend with $[1–3]\times10^{-3}$ °C yr^{-1} can be detected in the Niño3 and Niño3.4 region, while close to Indonesia and Australia a clear negative trend with the same magnitude appears. It corresponds to an increase of 0.15 to 0.45 °C in the SST variability, respectively, in 150 years (from 1950 to 2100), which is a considerable change compared to the magnitude

https://doi.org/10.5194/esd-2019-57
Preprint. Discussion started: 26 September 2019

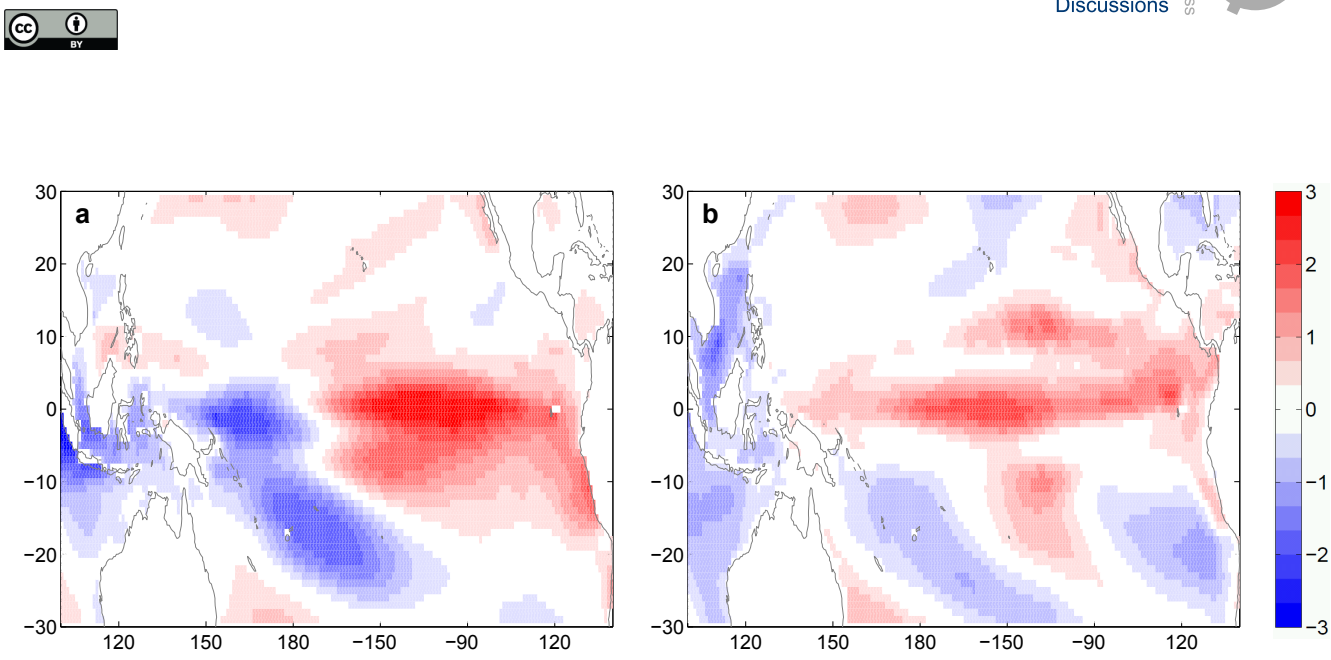

Figure 2. The slope of the linear fit [10^{-3} °C yr^{-1}] at each grid point of the (a) JJAS and (b) DJF regression maps from 1950 to 2100.

of 0.1–1 °C in the SST variability in Fig. 1. For DJF (Fig 2.b) a somewhat narrower band with slightly weaker increase of [0.5–2]$\times 10^{-3}$ °C yr^{-1} can be seen all along the Equator in the Pacific Ocean and negative trends in similar magnitude appear near Australia and at the western coast of South America. Similar trends in the annual ENSO pattern were pointed out in Maher et al. (2018), however, Fig. 2 draws attention to the fact that these patterns also have seasonal dependence.

Another particularly important feature of the ENSO phenomenon is the ENSO amplitude, which shows a large diversity in different climate projections (Yeh and Kirtman, 2007; Collins et al., 2010; Chen et al., 2015). Therefore, besides the exploration of the changes in the ENSO pattern, we also quantify the potential changes in the ENSO strength (the standard deviation of the PC1 (σ_{PC})) and the change in the explained variance of the first SEOF mode (Fig. 3.a,d, and b,e). Furthermore, the ensemble-based analog of a traditional amplitude of the ENSO phenomenon, namely, the Niño3 amplitude is also studied (Fig. 3.c, f). The value of σ_{PC} is much smaller in JJAS (Fig. 3.a) than in DJF (Fig. 3.d), and Fig 3.b and d also show that the explained variance in the SST variability by the first SEOF mode is about 15% greater in DJF than is JJAS. A systematic increase is found in all three quantities both for JJAS and for DJF. The increase in JJAS is around 20% in the σ_{PC} (Fig. 3.a), in the explained variance (Fig. 3.b), as well as in the ENSO amplitude (Fig. 3.c), while the increase in DJF is somewhat lower, approximately 5-15% for the three quantities. The approximately 20% increase in the Niño3 amplitude is in fairly good agreement with the study of Maher et al. (2018). It is comparable with the approximately 10% increase within 100 years in Zheng et al. (2018) found for the CESM-LE for the RCP8.5 scenario using sliding windows temporal statistics. This result reveals that the forced response of the ENSO amplitude under the climate change is positive. Obviously this finding is valid for the CESM-LE only, while other models may behave differently regarding the ENSO amplitude (Yeh and Kirtman, 2007; Kim et al., 2014; Chen et al., 2015). We mention that the first ensemble-based study (which investigated several large ensembles) reported that an increase or zero trend is likely regarding the Niño3 amplitude change (Maher et al., 2018).

https://doi.org/10.5194/esd-2019-57
Preprint. Discussion started: 26 September 2019

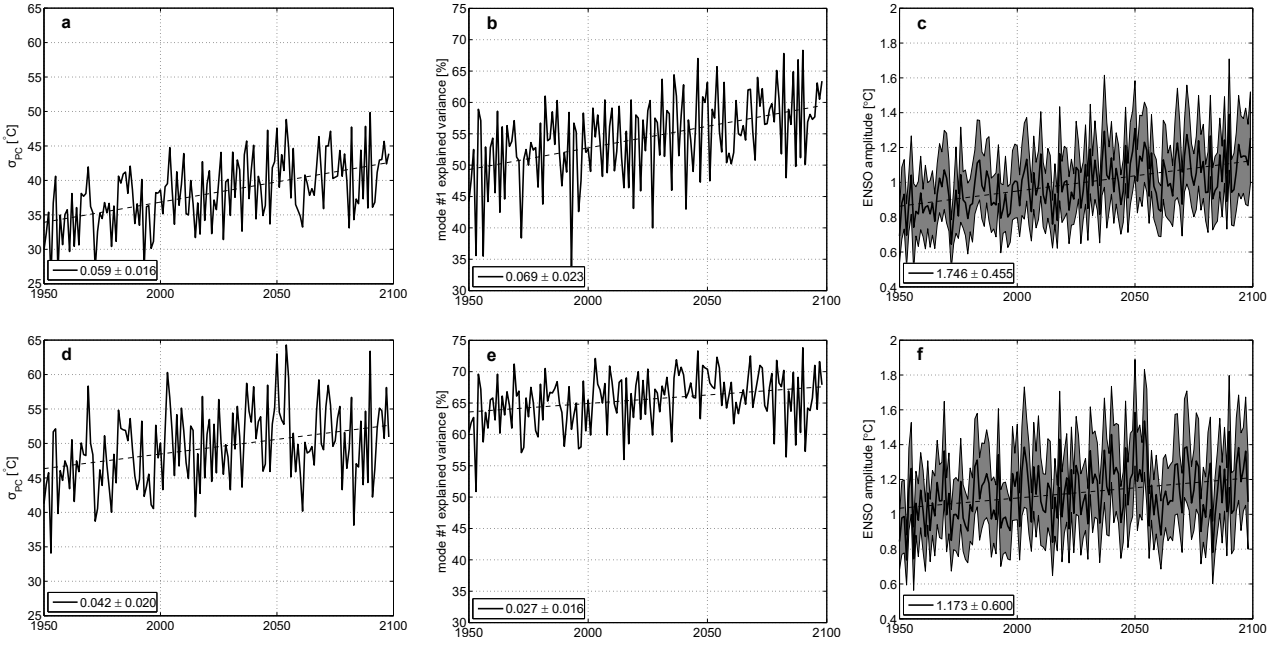

Figure 3. (a) and (d) ensemble-based ENSO strength as the standard deviation of the PC1 (σ_{PC}), (b) and (e) the explained variance of the first SEOF mode, and (c) and (f) Niño3 amplitude as the area-mean (thick line) ensemble standard deviation of SST in the Niño3 region and its area standard deviation (grey band)) in (a)-(c) JJAS and in (d)-(f) DJF. Linear fits are indicated by dashed lines, legends indicate the slope of the linear fits.

3.2 Changes in ENSO's teleconnections

To study the potential changes in the ENSO-related precipitation events, instantaneous ensemble-based correlation coefficients (r) between the PC1 and the total precipitation PRECT at each grid point is determined for both zero-lag and plus half-year-lagged PRECT data.

In Fig. 4 these r maps are presented. Four different combinations of PC1 and PRECT correlations are analyzed. The simultaneous (zero lag) correlation between the JJAS data in Fig 4.a-c shows that there are places where the correlation is remarkably negative, indicating dryer conditions during warm events and wetter weather during cold episodes. It is typically observable for Indonesia and Australia ($r \approx (-0.5) - (-0.8)$), East Africa ($r \approx (-0.4) - (-0.6)$), Central America ($r \approx (-0.4) - (-0.6)$), the northern part of South America ($r \approx -0.4.. - 0.6$), and southern and western part of India ($r \approx -0.4$). At the same time positive correlations, indicating more than average precipitation during El Niño and less than average for La Niña, can be seen for North Africa ($r \approx 0.4$) and the West Coast of the USA ($r \approx 0.3 - 0.6$). The above-presented picture is roughly consistent with observation-based investigations, see, e.g., Diaz et al. (2001).

It is worth assessing other variations of PC1 and PRECT correlations. The zero-lag correlation between DJF PC1 and DJF PRECT can be seen in Fig. 4.d-f. The anti-correlation with $r \approx (-0.4) - (-0.8)$ for South India, Indonesia and Australia still

https://doi.org/10.5194/esd-2019-57
Preprint. Discussion started: 26 September 2019

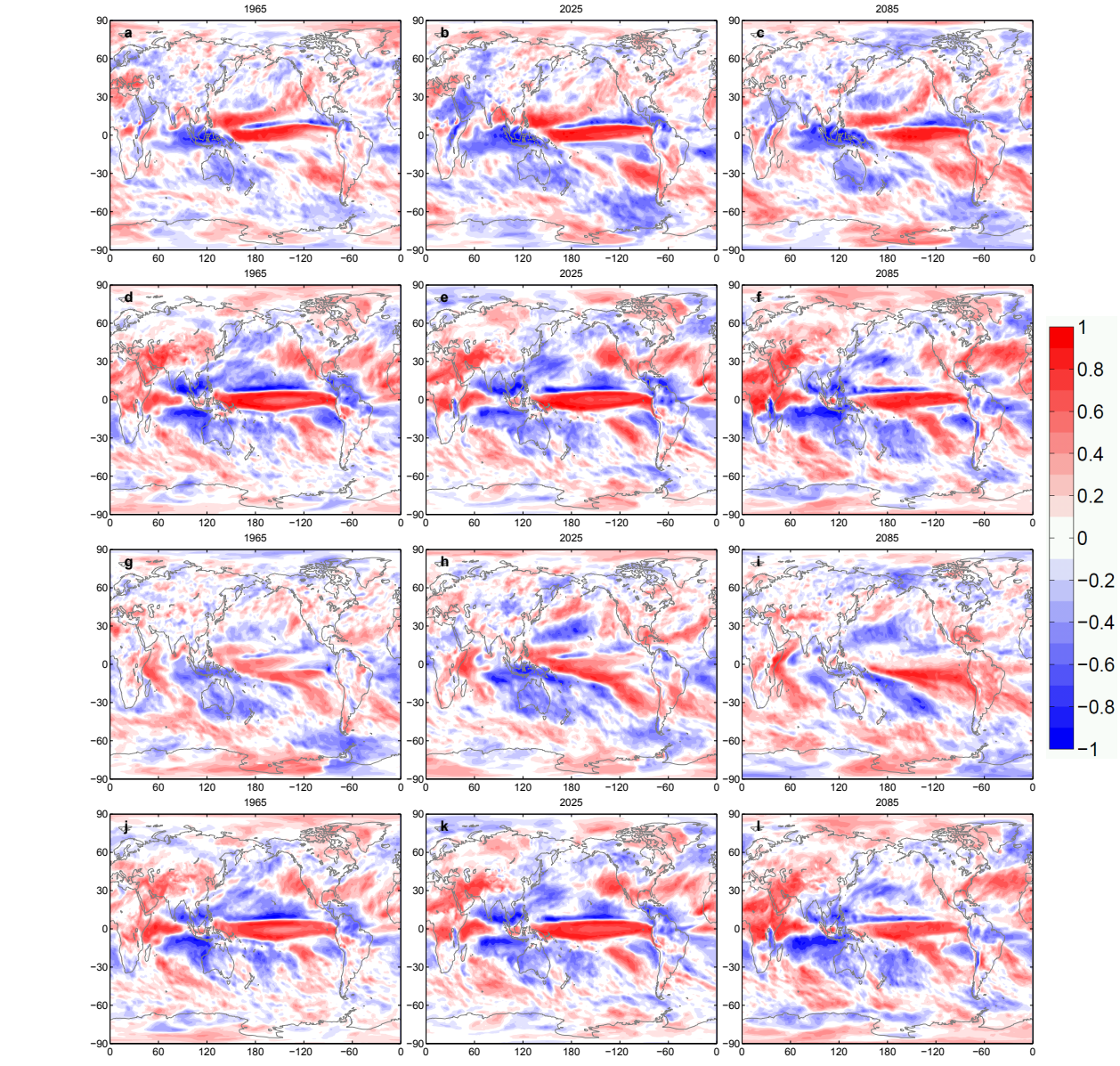

Figure 4. Ensemble based correlation coefficient r maps for the JJAS PC1 and JJAS PRECT (a-c), DJF PC1 and DJF PRECT (d-f), DJF PC1 and JJAS PRECT (g-i), JJAS PC1 and DJF PRECT (j-l). Specific years are indicated in the panels.

holds, as well as the positive correlation for the West Coast of the USA, while the East African correlation changes sign. In general, the DJF correlation patterns are also fairly close to the observation based ones, which was reported, e.g., in Diaz et al. (2001); Yang and DelSole (2012); Yeh et al. (2018).

https://doi.org/10.5194/esd-2019-57
Preprint. Discussion started: 26 September 2019


Earth System Dynamics Discussions

The role of the lagged correlations is also a relevant issue. It is known that lagged correlation is especially essential, e.g., for the Indian summer monsoon due to the potential monsoon forecasting (Wu et al., 2012; Johnson et al., 2017; Kucharski and Abid, 2017). Therefore, we construct the ensemble-based lagged correlation maps using the DJF PC1 and JJAS PRECT correlation (Fig. 4.g-i). The negative correlation appearing in observations for Indian JJAS precipitation with DJF ENSO phase (Wu et al., 2012) seems to be quite weak in CESM-LE, only a part of South India has some anti-correlation. This means that in CESM-LE the Indian summer monsoon does not seem to be predictable by the DJF PC1 of the ENSO. In contrast to this, as in the previous cases, the amount of the JJAS Indonesian and Australian precipitation shows a clear negative relationship with the DJF PC1. Examining the correlation between the JJAS PC1 and the following DJF PRECT we get interesting results (Fig. 4.j-l). India, the Indochinese Peninsula and Indonesia show a quite strong anti-correlation ($r \approx (-0.4) - (-0.8)$), while from the northern part of the Indian Ocean through the eastern and central part of Africa to northward to the Arabian Peninsula a considerable positive correlation can be observed. This suggests that based on the JJAS PC1, as an index for the actual ENSO phase, the DJF precipitation conditions are mostly predictable in these regions.

The question naturally arises, whether climate change has an impact on the strength of the teleconnections in these regions. To answer the question, similarly to the trends obtained for the regression maps in Fig. 2, we construct global linear trend maps of the correlation coefficient maps (Fig. 5). For the zero-lag correlations in JJAS (Fig. 5.a), among those regions where the strength of the connections are high during the investigated 150 years ($r > 0.4$ or $r < -0.4$, indicated by "+" and "." markers, respectively), Australia, an extended part of Indonesia and the southern part of South America show a clear increase of [1-2]$\times 10^{-3}$ yr^{-1} in the anti-correlation, while some spots in the southern part of the Atlantic Ocean and Central Africa have an increasing positive correlation during 1950–2100, that is, a strengthening of the connection between the phase of the ENSO and the precipitation conditions is found for these regions. South India's and Central America's positive correlation, the Phillipine Sea's negative correlation seem to weaken. For the zero-lag correlation in DJF (Fig. 5.b) a somewhat different picture opens up. The strength of the positive correlation from Central Africa to the Aral Sea and in the North Atlantic Ocean and the strength of the negative correlation in South India increase further by a trend of [1-4]$\times 10^{-3}$ yr^{-1}, and in the Niño3 region a somewhat stronger positive trend can be found than in JJAS. The spatial distribution of the correlation coefficients is similar for the JJAS PC1 and DJF PRECT (Fig. 2.d). The lagged correlations for DJF PC1 and JJAS PRECT (Fig. 5.c) are found to increase considerably near the eastern coast of Africa, in the Niño3 and Niño4 regions and around the Caribbean Islands. Thus, we conclude that a half-year-forward estimate of the precipitation from PC1 data in these regions becomes more accurate. The above-mentioned [1-4]$\times 10^{-3}$ yr^{-1} trends lead to a remarkable change of 0.15-0.45 in the r values during 150 years.

4 Conclusions

In this study, we investigated the changes in the ENSO phenomenon and the alterations of its precipitation-related teleconnections for 1950–2100 in the CESM-LE climate simulations. To avoid the disadvantages of the subjective choices of traditional temporal methods, here we used the ensemble-based snapshot framework providing instantaneous quantities computed over the ensemble dimension of the simulations. To our knowledge, this is the first time when the snapshot empirical orthogonal

https://doi.org/10.5194/esd-2019-57
Preprint. Discussion started: 26 September 2019

Earth System Dynamics
Discussions
Open Access
EGU

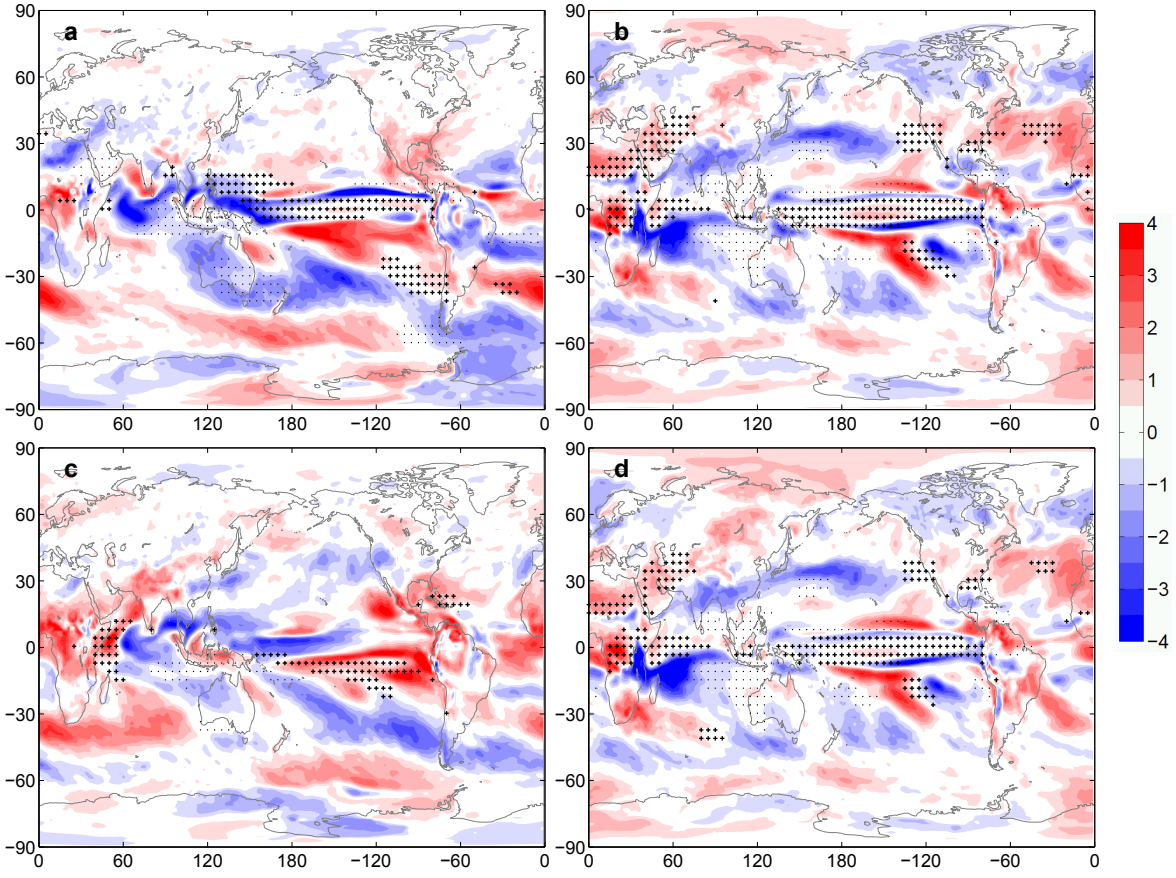

Figure 5. The slope of the linear fits [10^{-3} yr^{-1}] at each grid point for the correlation coefficient r for the JJAS PC1 and JJAS PRECT (a), DJF PC1 and DJF PRECT (b, DJF PC1 and JJAS PRECT (c), JJAS PC1 and DJF PRECT (d). Those grid points where the time average of r for 1950–2100 is below (above) -0.4 (0.4) are indicated by dots (plus signs).

function (SEOF) analysis using SST data is utilized to reveal changes in the pattern and amplitude of the ENSO. Instantaneous correlation coefficients between the principal components (PC1s) of the first SEOF mode (considered here as an index for the ENSO phase) and the total precipitation at each grid point over the Globe were also determined to evaluate the ENSO's precipitation-related teleconnections detailed below.

Our results show that the ENSO pattern undergoes remarkable changes during the investigated time period. This is found to be more pronounced in the JJAS season, where the SST regression maps show even 0.45 °C and -0.45 °C change in the Niño3–Niño3.4 region and in the western part of the Pacific Ocean, respectively. We note that these changes are of the same order of magnitude as the typical SST variability, which is found to be of 0.5–1.5 °C in the equatorial region. The Niño3 amplitude also increases by about 20% and 10% in JJAS and DJF, respectively. We found a clear growth of similar rate also in the ENSO strength (defined as the standard deviation of the PCs) and in the explained variance of the first SEOF mode. This

https://doi.org/10.5194/esd-2019-57
Preprint. Discussion started: 26 September 2019


Earth System Dynamics Discussions Open Access EGU

means that the amplitude of the fluctuations in the SST field will increase, and the first SEOF mode will explain a much larger fraction of the variability of the SST fields by the end of the 21th century.

The precipitation-related teleconnections of the ENSO also show a considerable change in several regions. For example, the anti-correlation with precipitation in Australia and in the southern edge of South America in JJAS are predicted to be more pronounced by the end of the 21th century, it changes from about -0.5 by -0.15. At the same time, the positive correlation in Central Africa and the western coast of South America, especially in Chile, becomes enhanced by $0.15 - 0.3$ as well.

Lagged correlation coefficients reveal potential predictability of the precipitation conditions based on ENSO's PC1. We found that the amount of precipitation in Australia, New Zealand, Indonesia in JJAS is generally less than average after DJF warm episodes, while, e.g., the eastern coast of Africa is wetter than average. In DJF the amount of precipitation in Australia and in South India is less than average after previous warm conditions in JJAS, however, the central islands in Indonesia and a large part of East and Central Africa get more precipitation. Our results show that the strength of these connections strengthens, especially in the African region up to the Arabian Peninsula, and slightly in South India.

We note that our method lacks any temporal statistics for the EOF analysis and correlation calculation for revealing teleconnections; thus, it is an objective way to explore the time evolution of other phenomena and teleconnections during climate change. Larger number of the ensemble members may even result in more accurate statistics and smaller fluctuations in the time series.

Code availability. Codes are available from T.H. on reasonable request.

Author contributions. T.H., M.H., T.B., conceived of the presented idea. M.H. downloaded and preprocessed the data, T.H. worked out the technical details, performed the computations and plotted the results. T.H. and M.H. took the lead in writing the manuscript. All authors discussed the results and contributed to the final manuscript.

Competing interests. The authors declare no competing interest.

Acknowledgements. Fruitful discussions with G. Drótos, T. Tél and M. Vincze are gratefully acknowledged. This paper was supported by the János Bolyai Research Scholarship of the Hungarian Academy of Sciences (T. H.), and by the National Research, Development and Innovation Office – NKFIH under grants PD-121305 (T. H.), PD-124272 (M. H.), FK-124256 and K-125171 (T. H., M. H.). The authors also wish to thank the Climate Data Gateway at NCAR for providing access to the output of the CESM-LE. The CESM-LE output is available at http://www.cesm.ucar.edu/projects/community-projects/LENS/data-sets.html.

https://doi.org/10.5194/esd-2019-57
Preprint. Discussion started: 26 September 2019

References

Arnold, L.: Random Dynamical Systems, Springer, Berlin, Heidelberg, 1998.

Ashok, K., Behera, S. K., Rao, S. A., Weng, H., and Yamagata, T.: El Niño Modoki and its possible teleconnection, Journal of Geophysical Research: Oceans, 112, 2007.

Bellenger, H., Guilyardi, É., Leloup, J., Lengaigne, M., and Vialard, J.: ENSO representation in climate models: from CMIP3 to CMIP5, Climate Dynamics, 42, 1999–2018, 2014.

Bittner, M., Schmidt, H., Timmreck, C., and Sienz, F.: Using a large ensemble of simulations to assess the Northern Hemisphere stratospheric dynamical response to tropical volcanic eruptions and its uncertainty, Geophysical Research Letters, 43, 9324–9332, https://doi.org/10.1002/2016GL070587, https://agupubs.onlinelibrary.wiley.com/doi/abs/10.1002/2016GL070587, 2016.

Bjerknes, J.: Atmospheric teleconnections from the equatorial Pacific, Monthly Weather Review, 97, 163–172, 1969.

Bódai, T. and Tél, T.: Annual variability in a conceptual climate model: Snapshot attractors, hysteresis in extreme events, and climate sensitivity, Chaos, 22, 023 110, https://doi.org/10.1063/1.3697984, 2012.

Bódai, T., Károlyi, G., and Tél, T.: Fractal snapshot components in chaos induced by strong noise, Phys. Rev. E, 83, 046 201, 2011.

Cai, W., Santoso, A., Wang, G., Yeh, S.-W., An, S.-I., Cobb, K. M., Collins, M., Guilyardi, E., Jin, F.-F., Kug, J.-S., et al.: ENSO and greenhouse warming, Nature Climate Change, 5, 849, 2015.

CESM-LE: LENS Known Issues, http://www.cesm.ucar.edu/projects/community-projects/LENS/known-issues.html, 2016.

Chekroun, M. D., Simonnet, E., and Ghil, M.: Stochastic climate dynamics: Random attractors and time-dependent invariant measures, Physica D: Nonlinear Phenomena, 240, 1685–1700, https://doi.org/10.1016/j.physd.2011.06.005, http://dx.doi.org/10.1016/j.physd.2011.06.005, 2011.

Chen, L., Li, T., and Yu, Y.: Causes of Strengthening and Weakening of ENSO Amplitude under Global Warming in Four CMIP5 Models, Journal of Climate, 28, 3250–3274, https://doi.org/10.1175/JCLI-D-14-00439.1, https://doi.org/10.1175/JCLI-D-14-00439.1, 2015.

Christensen, J. H., Kanikicharla, K. K., Marshall, G., and Turner, J.: Climate phenomena and their relevance for future regional climate change, in: Climate Change 2013: The physical science basis. Contribution of Working Group I to the fifth Assessment of the Intergovernmental Panel on Climate Change, edited by Stocker, T. F., Qin, D., Plattner, G.-K., Tignor, M. M., Allen, S. K., Boschung, J., Nauels, A., Xia, Y., Bex, V., and Midgley, P. M., pp. 1217–1308, Cambridge University Press, 2013.

Chung, E.-S., Timmermann, A., Soden, B. J., Ha, K.-J., Shi, L., and John, V. O.: Reconciling opposing Walker circulation trends in observations and model projections, Nature Climate Change, 9, 405–412, https://doi.org/10.1038/s41558-019-0446-4, https://doi.org/10.1038/s41558-019-0446-4, 2019.

Collins, M., An, S.-I., Cai, W., Ganachaud, A., Guilyardi, E., Jin, F.-F., Jochum, M., Lengaigne, M., Power, S., Timmermann, A., et al.: The impact of global warming on the tropical Pacific Ocean and El Niño, Nature Geoscience, 3, 391, 2010.

Daron, J. D. and Stainforth, D. A.: On predicting climate under climate change, Environmental Research Letters, 8, 034 021, https://doi.org/10.1088/1748-9326/8/3/034021, https://doi.org/10.1088%2F1748-9326%2F8%2F3%2F034021, 2013.

Davey, M., Brookshaw, A., and Ineson, S.: The probability of the impact of ENSO on precipitation and near-surface temperature, Climate Risk Management, 1, 5 – 24, https://doi.org/https://doi.org/10.1016/j.crm.2013.12.002, http://www.sciencedirect.com/science/article/pii/S2212096313000053, 2014.

Deser, C., Phillips, A., Bourdette, V., and Teng, H.: Uncertainty in climate change projections: the role of internal variability, Climate Dynamics, 38, 527–546, https://doi.org/10.1007/s00382-010-0977-x, https://doi.org/10.1007/s00382-010-0977-x, 2012.

https://doi.org/10.5194/esd-2019-57
Preprint. Discussion started: 26 September 2019

Diaz, H. F., Hoerling, M. P., and Eischeid, J. K.: ENSO variability, teleconnections and climate change, International Journal of Climatology, 21, 1845–1862, 2001.

Drótos, G., Bódai, T., and Tél, T.: Probabilistic Concepts in a Changing Climate: A Snapshot Attractor Picture, Journal of Climate, 28, 3275–3288, https://doi.org/10.1175/JCLI-D-14-00459.1, https://doi.org/10.1175/JCLI-D-14-00459.1, 2015.

Drótos, G., Bódai, T., and Tél, T.: Quantifying nonergodicity in nonautonomous dissipative dynamical systems: An application to climate change, Physical Review E, 94, 1–16, https://doi.org/10.1103/PhysRevE.94.022214, 2016.

Drótos, G., Bódai, T., and Tél, T.: On the importance of the convergence to climate attractors, European Physical Journal: Special Topics, 226, 2031–2038, https://doi.org/10.1140/epjst/e2017-70045-7, 2017.

Ghil, M., Chekroun, M. D., and Simonnet, E.: Climate dynamics and fluid mechanics: Natural variability and related uncertainties, Physica D: Nonlinear Phenomena, 237, 2111–2126, https://doi.org/10.1016/j.physd.2008.03.036, 2008.

Glantz, M. H., Glantz, M. H., et al.: Currents of change: impacts of El Niño and La Niña on climate and society, Cambridge University Press, 2001.

Guilyardi, E., Wittenberg, A., Fedorov, A., Collins, M., Wang, C., Capotondi, A., Van Oldenborgh, G. J., and Stockdale, T.: Understanding El Niño in ocean–atmosphere general circulation models: Progress and challenges, Bulletin of the American Meteorological Society, 90, 325–340, 2009.

Haszpra, T., Topál, D., and Herein, M.: On the time evolution of the Arctic Oscillation and related wintertime phenomena under different forcing scenarios in an ensemble approach, Journal of Climate (under review), 2019.

Hedemann, C., Mauritsen, T., Jungclaus, J., and Marotzke, J.: The subtle origins of surface-warming hiatuses, Nature Climate Change, 7, 336 EP –, https://doi.org/10.1038/nclimate3274, 2017.

Herein, M., Márfy, J., Drótos, G., and Tél, T.: Probabilistic concepts in intermediate-complexity climate models: A snapshot attractor picture, Journal of Climate, 29, 259–272, https://doi.org/10.1175/JCLI-D-15-0353.1, 2016.

Herein, M., Drótos, G., Haszpra, T., Márfy, J., and Tél, T.: The theory of parallel climate realizations as a new framework for teleconnection analysis, Scientific Reports, 7, 44 529, https://doi.org/10.1038/srep44529, http://www.nature.com/articles/srep44529, 2017.

Johnson, S. J., Turner, A., Woolnough, S., Martin, G., and MacLachlan, C.: An assessment of Indian monsoon seasonal forecasts and mechanisms underlying monsoon interannual variability in the Met Office GloSea5-GC2 system, Climate Dynamics, 48, 1447–1465, https://doi.org/10.1007/s00382-016-3151-2, https://doi.org/10.1007/s00382-016-3151-2, 2017.

Kay, J. E., Deser, C., Phillips, A., Mai, A., Hannay, C., Strand, G., Arblaster, J. M., Bates, S. C., Danabasoglu, G., Edwards, J., Holland, M., Kushner, P., Lamarque, J.-F., Lawrence, D., Lindsay, K., Middleton, A., Munoz, E., Neale, R., Oleson, K., Polvani, L., and Vertenstein, M.: The Community Earth System Model (CESM) Large Ensemble Project: A Community Resource for Studying Climate Change in the Presence of Internal Climate Variability, Bulletin of the American Meteorological Society, 96, 1333–1349, https://doi.org/10.1175/BAMS-D-13-00255.1, 2015.

Kim, S., Cai, W., Jin, F., Santoso, A., Wu, L., Guilyardi, E., and An, S.-I.: Response of El Niño sea surface temperature variability to greenhouse warming, Nature Climate Change, 4, 786–790, https://doi.org/10.1038/nclimate2326, 2014.

Kirtman, B. P. and Shukla, J.: Influence of the Indian summer monsoon on ENSO, Quarterly Journal of the Royal Meteorological Society, 126, 213–239, https://doi.org/10.1002/qj.49712656211, https://rmets.onlinelibrary.wiley.com/doi/abs/10.1002/qj.49712656211, 2000.

Kucharski, F. and Abid, M. A.: Interannual Variability of the Indian Monsoon and Its Link to ENSO, https://oxfordre.com/climatescience/view/10.1093/acrefore/9780190228620.001.0001/acrefore-9780190228620-e-615, 2017.

https://doi.org/10.5194/esd-2019-57
Preprint. Discussion started: 26 September 2019

Kumar, K. K., Rajagopalan, B., and Cane, M. A.: On the Weakening Relationship Between the Indian Monsoon and ENSO, Science, 284, 2156–2159, https://doi.org/10.1126/science.284.5423.2156, https://science.sciencemag.org/content/284/5423/2156, 1999.

Lamarque, J.-F., Bond, T. C., Eyring, V., Granier, C., Heil, A., Klimont, Z., Lee, D., Liousse, C., Mieville, A., Owen, B., Schultz, M. G., Shindell, D., Smith, S. J., Stehfest, E., Van Aardenne, J., Cooper, O. R., Kainuma, M., Mahowald, N., McConnell, J. R., Naik, V., Riahi, K., and van Vuuren, D. P.: Historical (1850–2000) gridded anthropogenic and biomass burning emissions of reactive gases and aerosols: methodology and application, Atmospheric Chemistry and Physics, 10, 7017–7039, https://doi.org/10.5194/acp-10-7017-2010, https://www.atmos-chem-phys.net/10/7017/2010/, 2010.

Leith, C.: Predictability of climate, Nature, 276, 352, 1978.

Li, H. and Ilyina, T.: Current and Future Decadal Trends in the Oceanic Carbon Uptake Are Dominated by Internal Variability, Geophysical Research Letters, 45, 916–925, https://doi.org/10.1002/2017GL075370, https://agupubs.onlinelibrary.wiley.com/doi/abs/10.1002/2017GL075370, 2018.

Maher, N., Matei, D., Milinski, S., and Marotzke, J.: ENSO change in climate projections: forced response or internal variability?, Geophysical Research Letters, 45, 11–390, 2018.

Neelin, J. D., Battisti, D. S., Hirst, A. C., Jin, F.-F., Wakata, Y., Yamagata, T., and Zebiak, S. E.: ENSO theory, Journal of Geophysical Research: Oceans, 103, 14 261–14 290, 1998.

Philander, S. G.: El Niño, La Niña, and the Southern Oscillation, Tech. rep., 1990.

Ramu, D. A., Chowdary, J. S., Ramakrishna, S. S. V. S., and Kumar, O. S. R. U. B.: Diversity in the representation of large-scale circulation associated with ENSO-Indian summer monsoon teleconnections in CMIP5 models, Theoretical and Applied Climatology, 132, 465–478, https://doi.org/10.1007/s00704-017-2092-y, https://doi.org/10.1007/s00704-017-2092-y, 2018.

Rasmusson, E. M. and Carpenter, T. H.: Variations in tropical sea surface temperature and surface wind fields associated with the Southern Oscillation/El Niño, Monthly Weather Review, 110, 354–384, 1982.

Romeiras, F. J., Grebogi, C., and Ott, E.: Multifractal properties of snapshot attractors of random maps, Physical Review A, 41, 784–799, https://doi.org/10.1103/PhysRevA.41.784, 1990.

Roy, I., Tedeschi, R. G., and Collins, M.: ENSO teleconnections to the Indian summer monsoon under changing climate, International Journal of Climatology, 39, 3031–3042, 2019.

Stevens, B.: Rethinking the Lower Bound on Aerosol Radiative Forcing, Journal of Climate, 28, 4794–4819, https://doi.org/10.1175/JCLI-D-14-00656.1, 2015.

Stevenson, S.: Significant changes to ENSO strength and impacts in the twenty-first century: Results from CMIP5, Geophysical Research Letters, 39, 2012.

Suarez-Gutierrez, L., Li, C., Müller, W. A., and Marotzke, J.: Internal variability in European summer temperatures at 1.5°C and 2°C of global warming, Environmental Research Letters, 13, 064 026, https://doi.org/10.1088/1748-9326/aaba58, 2018.

Takahashi, K., Montecinos, A., Goubanova, K., and Dewitte, B.: ENSO regimes: Reinterpreting the canonical and Modoki El Niño, Geophysical Research Letters, 38, 2011.

Taylor, K. E., Stouffer, R. J., and Meehl, G. A.: An overview of CMIP5 and the experiment design, Bulletin of the American Meteorological Society, 93, 485–498, 2012.

Thompson, D. W. and Wallace, J. M.: Annular modes in the extratropical circulation. Part I: Month-to-month variability, Journal of climate, 13, 1000–1016, 2000.

https://doi.org/10.5194/esd-2019-57
Preprint. Discussion started: 26 September 2019

Timmermann, A., An, S.-I., Kug, J.-S., Jin, F.-F., Cai, W., Capotondi, A., Cobb, K. M., Lengaigne, M., McPhaden, M. J., Stuecker, M. F., et al.: El Niño–Southern Oscillation complexity, Nature, 559, 535, 2018.

Trenberth, K. E., Branstator, G. W., Karoly, D., Kumar, A., Lau, N.-C., and Ropelewski, C.: Progress during TOGA in understanding and modeling global teleconnections associated with tropical sea surface temperatures, Journal of Geophysical Research: Oceans, 103, 14 291–14 324, 1998.

Trenberth, K. E., Caron, J. M., Stepaniak, D. P., and Worley, S.: Evolution of El Niño–Southern Oscillation and global atmospheric surface temperatures, Journal of Geophysical Research: Atmospheres, 107, AAC–5, 2002.

Tél, T., Bódai, T., Drótos, G., Haszpra, T., Herein, M., Kaszás, B., and Vincze, M.: The theory of parallel climate realizations: A new framework of ensemble methods in a changing climate -– an overview, Submitted to Journal of Statistical Physics, 2019.

Van Vuuren, D. P., Edmonds, J., Kainuma, M., Riahi, K., Thomson, A., Hibbard, K., Hurtt, G. C., Kram, T., Krey, V., Lamarque, J.-F., et al.: The representative concentration pathways: an overview, Climatic change, 109, 5, 2011.

Vecchi, G. A. and Wittenberg, A. T.: El Niño and our future climate: Where do we stand?, Wiley Interdisciplinary Reviews: Climate Change, 1, 260–270, 2010.

Vincze, M., Borcia, I. D., and Harlander, U.: Temperature fluctuations in a changing climate: an ensemble-based experimental approach, Scientific Reports, 7, 254, https://doi.org/10.1038/s41598-017-00319-0, http://www.nature.com/articles/s41598-017-00319-0, 2017.

Wallace, J., Rasmusson, E., Mitchell, T., Kousky, V., Sarachik, E., and Von Storch, H.: On the structure and evolution of ENSO-related climate variability in the tropical Pacific: Lessons from TOGA, Journal of Geophysical Research: Oceans, 103, 14 241–14 259, 1998.

Wu, R., Chen, J., and Chen, W.: Different Types of ENSO Influences on the Indian Summer Monsoon Variability, Journal of Climate, 25, 903–920, https://doi.org/10.1175/JCLI-D-11-00039.1, https://doi.org/10.1175/JCLI-D-11-00039.1, 2012.

Yang, X. and DelSole, T.: Systematic Comparison of ENSO Teleconnection Patterns between Models and Observations, Journal of Climate, 25, 425–446, https://doi.org/10.1175/JCLI-D-11-00175.1, https://doi.org/10.1175/JCLI-D-11-00175.1, 2012.

Yeh, S.-W. and Kirtman, B. P.: ENSO amplitude changes due to climate change projections in different coupled models, Journal of climate, 20, 203–217, 2007.

Yeh, S.-W., Cai, W., Min, S.-K., McPhaden, M. J., Dommenget, D., Dewitte, B., Collins, M., Ashok, K., An, S.-I., Yim, B.-Y., et al.: ENSO atmospheric teleconnections and their response to greenhouse gas forcing, Reviews of Geophysics, 56, 185–206, 2018.

Zheng, X.-T., Hui, C., and Yeh, S.-W.: Response of ENSO amplitude to global warming in CESM large ensemble: uncertainty due to internal variability, Climate dynamics, 50, 4019–4035, 2018.